Biomaterials Science

ECM proteins and cationic polymers coating promote dedifferentiation of patient-derived mature adipocytes to stem cells

Journal:	*Biomaterials Science*
Manuscript ID	BM-ART-05-2023-000934.R1
Article Type:	Paper
Date Submitted by the Author:	21-Sep-2023
Complete List of Authors:	Karanfil, Aslı; Osaka University, Applied Chemistry Louis, Fiona; Osaka University, Joint Research Laboratory (TOPPAN) for Advanced Cell Regulatory Chemistry, Graduate School of Engineering Sowa, Yoshihiro; Kyoto Prefectural University of Medicine, Department of Plastic and Reconstructive Surgery; Kyoto University Graduate School of Medicine Faculty of Medicine, Department of Plastic and Reconstructive Surgery Matsusaki, Michiya; Osaka University, Graduate School of Engineering, Department of Applied Chemistry

ARTICLE

ECM proteins and cationic polymers coating promote dedifferentiation of patient-derived mature adipocytes to stem cells

Received 00th January 20xx,
Accepted 00th January 20xx

DOI: 10.1039/x0xx00000x

Aslı Sena Karanfil[a], Fiona Louis[b*], Yoshihiro Sowa[c,d] and Michiya Matsusaki[a,b*]

Reprogramming of mature adipocytes is an attractive research area due to the plasticity of these cells. Mature adipocytes can be reprogrammed *in vitro*, transforming them into dedifferentiated fat cells (DFATs), which are considered a new type of stem cell, and thereby have a high potential for use in tissue engineering and regenerative medicine. However, there are still no reports or findings on *in vitro* controlling the dedifferentiation. Although ceiling culture performed in related studies is a relatively simple method, its yield is low and does not allow manipulation of mature adipocytes to increase or decrease the dedifferentiation. In this study, to understand the role of physicochemical surface effects on the dedifferentiation of patient-derived mature adipocytes, the surfaces of cell culture flasks were coated with extracellular matrix, basement membrane proteins, and cationic/anionic polymers. Extracellular matrix such as fibronectin and collagen type I, and basement membrane proteins such as collagen type IV and laminin strongly promoted dedifferentiation of mature adipocytes, with laminin showing the highest effect with a DFAT ratio of 2.98 (± 0.84). Interestingly, cationic polymers also showed a high dedifferentiation effect, but anionic polymers did not, and poly(diallyl dimethylammonium chloride) showed the highest DFAT ratio of 2.27 (± 2.8) among the cationic polymers. Protein assay results revealed that serum proteins were strongly adsorbed on the surfaces of the cationic polymer coating, including inducing high mature adipocyte adhesion. This study demonstrates for the first time the possibility of regulating the transformation of mature adipocytes to DFAT stem cells by controlling the physicochemical properties of the surface of conventional cell culture flasks.

1. Introduction

Adipose tissue (AT) and adipocytes (fat tissue cells) have been an attractive research area for many years, as obesity and related comorbidities continue to be important health problems. AT is a unique tissue that makes up 10-30% of body weight and regulates body homeostasis with various endocrine and secretion functions that affect insulin sensitivity, lipid metabolism and satiety.[1–3] Mature adipocytes, the main cellular component of AT, are in a spherical form that can expand up to a cell diameter of 290 microns, surrounded by smaller preadipocytes, nerves and capillaries that fill the interstitial spaces, arranged in a honeycomb-like geometry.[4] These cells have high plasticity and their ability to reprogram themselves both *in vivo* and *in vitro* in response to a variety of pathological and physiological cues makes them unique.[5] They can also dedifferentiate into cells with highly proliferative activity and the ability to differentiate into various cell types in cell culture conditions.[6,7] These cells, called dedifferentiated fat cells (DFATs), lose the lipid content of mature adipocytes and gain multipotent properties with a spindle-shaped morphology.[8] Their potential to differentiate into other cell types when the required culture conditions are provided and their relatively easy availability compared to other stem cell types make them an advantageous resource for tissue engineering, regenerative medicine, cell therapy and stem cell research. For example, mesenchymal stem cells (MSCs) isolated by the bone marrow procedure which is a highly invasive and complex process, represent only around 0.01-0.001% of nucleated cells in adult human bone marrow with a relatively low yield.[9] However, the percentage of stem cells by using AT ranges from 1% to 10%, resulting in a possible total range for adipose-derived stem cells from 5,000 to 200,000 cells per mL that can be isolated from adipose tissue stromal vascular fraction (SVF).[10] In comparison, DFAT isolation yield is potentially higher, since it can be attributed to the fact that DFAT cells are derived from mature adipocytes, which constitute 15-30% of the total adipose cell fraction.[11] Therefore, using DFATs might be more advantageous because of the stem cell yields and, relatedly, it has been reported that 3×10^7 DFAT can be

[a.] *Department of Applied Chemistry, Graduate School of Engineering, Osaka University, Japan. E-mail: m-matsus@chem.eng.osaka-u.ac.jp*
[b.] *Joint Research Laboratory (TOPPAN) for Advanced Cell Regulatory Chemistry, Graduate School of Engineering, Osaka University, Japan*
[c.] *Department of Plastic and Reconstructive Surgery, Graduate School of Medical Sciences, Kyoto Prefectural University of Medicine, Japan.*
[d.] *Department of Plastic and Reconstructive Surgery, Graduate School of Medicine, Kyoto University, Japan.*
† Footnotes relating to the title and/or authors should appear here.
Electronic Supplementary Information (ESI) available: [details of any supplementary information available should be included here]. See DOI: 10.1039/x0xx00000x

obtained after several passages from 5×10^4 mature adipocytes isolated from 1 g of AT in primary culture.[6] Therefore, compared to other multipotent stem cells, DFATs might have advantages over other stem cell types, as they can be easily and abundantly obtained from waste AT obtained by methods such as liposuction. Both ADSC and DFAT are stem cells derived from adipose tissue, but they have distinct characteristics and origins. ADSC derived from the stromal vascular fraction of adipose tissue, while DFAT cells are generated by dedifferentiating mature adipocytes. These DFAT cells exhibit comparable surface markers to ADSC, including CD105, CD73, and CD90. However, they might also show the presence of certain markers, such as CD36 and CD10, which are not commonly observed in other MSCs.[12] Based on prior research and our own findings, it appears that DFATs exhibit similar capabilities for multilineage differentiation and stemness as ADSCs. While both cell types share highly comparable characteristics, a few studies have suggested slight disparities between them. Watson et al. demonstrated through RT-PCR analysis that ADSCs express slightly higher levels of embryonic-related stemness markers, namely BMI1 and KLF4. In contrast, flow cytometry analysis revealed that DFATs have a slightly higher CD31 expression compared to ADSCs, with percentages of 8.3% and 1.1%, respectively. Their report also highlights the most significant difference between the two cell types, which is the increased levels of telomerase and enhanced capacity for redifferentiation and transdifferentiation into adipocytes and osteoblasts observed in DFATs compared to ADSCs. DFATs were reported to have 2.5 times more telomerase activity than ADSCs.[13] In summary, one of the DFAT values is that they may be potentially more versatile for certain regenerative medicine applications. Consequently, these highly proliferating cells can be differentiated into several cell lineages, such as osteogenic, chondrogenic and adipogenic lineages similar to SVFs.[6,7] DFATs have been reported to be differentiated into peripheral nerve[14], skeletal muscle[15], cartilage[16], bone[17], and fat[18] cells *in vitro*. However, despite their high potential, there are several factors that make the primary culture of mature adipocytes challenging. First, since they have a high cytoplasmic lipid content of around 90%, they have low density and are highly buoyant. Therefore, they cannot be cultured by cellular adhesion on the bottom surface of cell culture dishes with traditional cell culture methods.[4] Up to now, various specific culture methods have been developed that allow the culture and dedifferentiation of mature adipocytes.[19–21] In ceiling culture, first presented by Sugihara et al. in 1986, cell culture flasks are completely filled with cell culture medium, allowing mature adipocytes to be attached to the ceiling of the flasks.[19] Adhered cells lose their cytoplasmic fat content within a few days, gain a fibroblastic appearance and DFATs are obtained. In another method, a glass coverslip is placed on the freshly isolated mature adipocytes, so that the cells adhere to the coverslip surface and are dedifferentiated.[20,22] In current studies investigating the chemical, biological and physiological factors underlying the mechanism of mature adipocyte dedifferentiation, it has been reported that the YAP/TAZ, Hippo, Hedgehog, and PPARγ signaling pathways play a role by reorganizing the cytoskeleton.[23,24] To date, various factors such as the oxygen content of the medium[25] and the stiffness of the substrate[23] have been emphasized in studies investigating the causes of dedifferentiation of mature adipocytes. Although the dedifferentiation mechanism within them has not been fully elucidated, several related reports have confirmed that substrate stiffness might be one of the important factors.[23,26,27] In the microfluidic system demonstrated by Kim et al., which provides the opportunity to observe the dedifferentiation mechanism in detail, it has been shown that actin myofibrils reorganize the cytoskeleton of the actin myofibrils and expel the lipid droplet from the cell, making the cells acquire a fibroblastic morphology while turning into DFATs.[24] This study also showed that coating with fibronectin on the surface promotes adipocyte dedifferentiation. Based on the related literature, we aimed to further control and improve the dedifferentiation ratio of mature adipocytes by using cationic and anionic polymers, and proteins which are the main components of the tissue extracellular matrix (ECM) and basement membrane (BM). First, we focused on increasing the cell adhesion and dedifferentiation due to the interaction of integrin molecules, which allow cells to adhere to the surface, ECM and BM components. Second, we decided to increase the cell culture flask surface adsorption of vitronectin and fibronectin proteins, also known as cell adhesion factors in serum[28,29], by coating the flask surfaces with positively charged polymers to increase cell adhesion and thus dedifferentiation. Finally, we confirmed the DFAT-increasing effect of cationic polymers by coating cell culture flasks with anionic polymers.

2. Materials and methods

2.1 Chemicals and reagents

Collagen type IV (from human placenta, C7521), Fibronectin (from human plasma, F2006), Poly-L-lysin (PLL, P4707), Poly(allylamine) (PAH, 479136), Poly(diallyldimethylammonium chloride) (PDDA, 26062-79-3), Collagenase (from Clostridium histolyticum, type I, C0130), Triton-X 100 (T8787), Collagen type I-FITC conjugated from bovine skin (C4361), Poly-L-lysine-FITC conjugated (P3543), CD90 (Anti-THY1) primary antibody (HPA003733), and Bovine Serum Albumin (BSA, 3294), Alcian Blue 8GX solution (1003580143), and Oil Red O (O0625) were purchased from Sigma-Aldrich (St Louis, MO, USA). Collagen type IV-FAM conjugated (AS-85112) obtained from AnaSpec (California, USA). Rhodamine Laminin (LMN01-A), and Rhodamine Fibronectin (FNR01-A) obtained from Cytoskeleton, Inc. (Denver, USA), YAP primary antibody (sc-101199) obtained from Santa Cruz (Texas, USA). Hoechst 33324 (H3570), Trypan Blue (T10282), Pierce™ BCA protein assay kit (23225), Oct-4 Monoclonal Antibody (MA1-104), StemPro™ Osteogenesis Differentiation Kit (A1007201), and StemPro™ Chondrogenesis Differentiation Kit (A1007101) were purchased from ThermoFisher Scientific (Whaltam, MA, USA), Invitrogen. Human Adipogenic Differentiation Medium (811D-250) obtained from Cell Applications, Inc. (San Diego, USA). Phosphate Buffer Saline (D-PBS, 14249-24) and Dulbecco's Modified Eagle Medium (DMEM) high glucose (08458-16) came from Nacalai Tesque Inc. (Kyoto, Japan). Fetal Bovine Serum (FBS, 10270106) were obtained from Gibco. Phalloidin-iFluor 594 Reagent (ab176757)

purchased from Abcam (Cambridge, UK). Trypsin (207192-83), Gelatin (077-03155) and Alizarin Red S (011-01192) came from Wako Pure Chemical Industries (Tokyo, Japan). Live/Dead® viability assay kit (PK-CA707-30002) purchased from PromoKine (Heidelberg, Germany), T12.5 cell culture flasks (353018) and Laminin (354259) obtained from Corning (Arizona, USA). Collagen type I (from bovine dermis, Atelocell, IPC-50) from Koken (Tokyo, Japan). Gellan Gum (8H1121A) came from Sansho (Osaka, Japan). APC anti human CD105 (323207), APC anti-human CD90 (328113), APC anti-human CD73 (344005), APC/Cyanine7 Mouse IgG2b, κ Isotype Ctrl (402210) purchased from BioLegend (San Diego, California, USA). APC anti human CD44 (560532) obtained from BD Biosciences (New Jersey, USA).

2.2 Experimental section

2.2.1 Isolation of mature adipocytes

Human ATs from patients were isolated at Kyoto University Hospital. Before the mature adipocyte isolation, tissues were washed with PBS containing 5% of Penicillin-Streptomycin. Then, 2-3 g of AT were inserted into each well of a 6-well plate and minced to obtain around 1 mm^3 by using autoclaved tweezers and scissors. 2 mL of collagenase solution at 2 mg/mL in DMEM 0% FBS, 5% BSA and 1% Penicillin-Streptomycin (sterilized by filtration) was directly added onto each well and incubated for 1 h at 37°C with 250 rpm rotation. After incubation, the lysate was filtrated using a 500 µm pore size filter and centrifuged for 3 min at 80g. After centrifugation, mature adipocytes were found floating on the top layer of the tube, while stromal vascular fraction were on the bottom of the tube. The liquid between the top layer and pellet was discarded by 10 mL pipette and washing was repeated two times with PBS with 5% BSA and 1% Penicillin-Streptomycin with a final wash in DMEM. Freshly isolated mature adipocytes were used for all ceiling culture experiments.

One of the important factors that makes *in vitro* studies performed with adipocyte challenging is the difficulty in obtaining fully reproducible results in cell culture experiments performed with isolated cells depending on sex, age, fat mass, anatomical location, and pathophysiological condition of the donor.[30] Therefore, we conducted this study with AT samples taken from three different patients. It has also been reported that there is a decrease in the proliferative activity of DFATs obtained from patients aged 70 years and older.[6] Indeed, our own experiments confirmed this finding (data not shown).

Ethics statement: The adipose tissues were collected from Kyoto University Hospital (Kyoto, Japan) after abdominal adipose tissue or liposuction isolation of three human donors aged 41, 45, and 53 years old, with a BMI of 22.40, 25.78, and 20.46, respectively. All experiments were performed in accordance with the Guidelines of Kyoto University, and Experiments were approved by the Osaka University Research Ethics Review Committee (approval number: L026). Informed consents were obtained from human participants of this study.

2.2.2 Serum protein effect assessment of DFAT ratio

Mature adipocytes were seeded with a seeding density of $5.0\times10^4/cm^2$ in uncoated poly styrene (PS) cell culture flasks that were fully filled by DMEM including 20%, 10% and 0% of FBS with 1% of Penicillin-Streptomycin. Each flask was tightly capped to prevent medium leakage and incubated at 37°C for 1 week. After incubation, the medium was aspirated, obtained DFATs were detached by trypsinization and cells were counted with an automated cell countess (Invitrogen), by using Trypan Blue. To normalize the data, the counted DFATs number obtained by DMEM including 0% FBS was used as a control to compare the other condition's cell number.

2.2.3 Cell viability assay

The viability of cells cultured in ceiling cultures for 1 week with DMEM including 20%, 10% and 0% PBS (v/v) were evaluated using a Live/Dead® viability assay kit. In addition, to evaluate cytotoxicity of PAH coating, PS cell culture surfaces were coated with PAH, then DFATs were seeded as the cell density $1.2x10^4/cm^2$. Next, Live/Dead staining was carried out on day 7 and compared with uncoated PS surface. Nuclei of cells were counterstained with Hoechst. After washing with PBS three times, the cells on the surface were stained (green: living cells, red: dead cells, blue: nuclei) for 30 min at 37°C in the dark, then imaged by an FV3000 Confocal Laser Scanning Microscope (Olympus, Tokyo, Japan).

2.2.4 Immunofluorescence imaging of DFATs

After 1 week of ceiling culture with uncoated PS flasks, DFATs were detached and seeded onto 10 cm petri dishes and cultured on the dishes until reaching 80% of confluence. The cells were then detached again and seeded onto a 96 well plate with 1.2×10^4 seeding density. After the cells reached confluence, they were fixed with 4% paraformaldehyde solution in PBS overnight at 4°C. Samples were permeabilized in 0.05% Triton X-100 in PBS for 15 min and incubated for 1 h at room temperature in 1% BSA in PBS to minimize non-specific staining. Anti-CD90 and Anti-YAP antibodies were added in BSA 1% and incubated overnight at 4°C. Then, samples were incubated with secondary antibodies Alexa Fluor® 647 and Alexa Fluor® 488 at room temperature in the dark for 2 h. Subsequently, F-actin (CytoPainter Phalloidin-iFluor 594 reagent) staining were carried out following the manufacturer's guide. Nuclei were counterstained with Hoechst. In addition, DFATs were seeded into another 96 well plate and were incubated with Oct-4 primary antibody (MA1-104, Thermofisher) in BSA 1% and incubated 1 h at room temperature. Then, samples were incubated with secondary Alexa Fluor® 488 at room temperature in the dark for 2 h. Then, same F-actin and Hoechst staining steps were performed. The cells were rinsed in PBS and observed using an FV3000 Confocal Laser Scanning Microscope (Olympus, Tokyo, Japan).

2.2.5 Multilineage differentiation of DFATs

To test multilineage differentiation ability of DFATs, cells were differentiated into osteoblast, chondroblast and adipocytes. For osteogenic and chondrogenic differentiation, DFATs were seeded

onto 24-well plate with 5.0x10^3 seeding density. After cells reach approximately 80% confluency, they were cultured in StemPro™ Osteogenesis and Chondrogenesis kits by following to manufacturer's protocols. For adipogenic differentiation, cells were seeded onto 24-well plate with 1.2x10^4 seeding density and cultured with Adipocyte Differentiation Medium (Cell application, Inc). Alizarin Red S, Alcian Blue and Oil Red O staining performed to confirm osteogenic on day 21, chondrogenic on day 14 and adipogenic differentiation status on day 14, respectively.

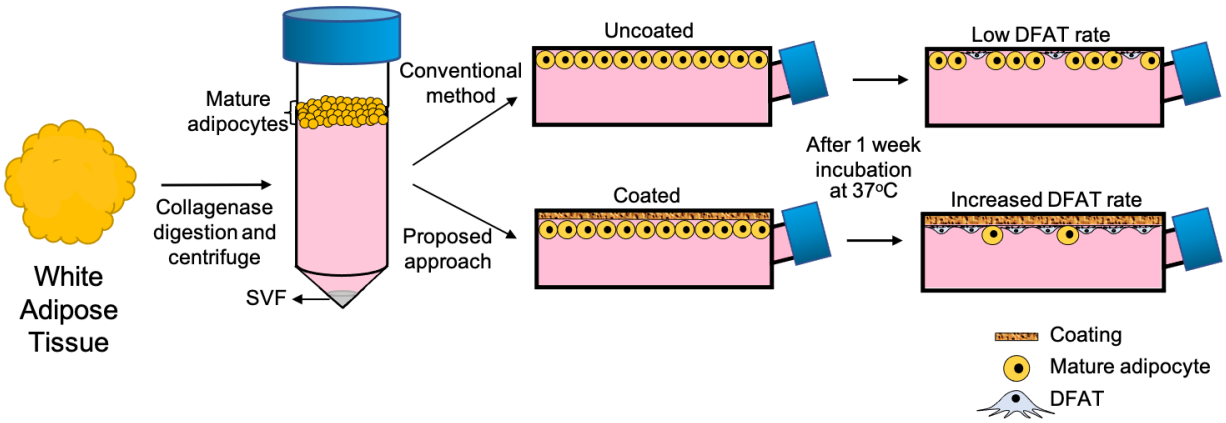

Fig. 1 Schematic illustration of improved ceiling culture method to increase dedifferentiated fat (DFAT) cell rate by extracellular matrix, basement membrane and cationic/anionic polymer coating on the inner top surface of the cell culture flasks..

2.2.6 Ceiling culture with coated cell culture flasks

Mature adipocytes were seeded with a seeding density of 5.0×10^4/cm^2 in protein and polymer coated PS flasks that were fully filled by DMEM including 20% of FBS with 1% of Penicillin-Streptomycin. Each flask was tightly capped to prevent medium leakage and incubated at 37°C for 1 week. After incubation, the medium was aspirated, obtained DFATs were detached by trypsinization and cells were counted with an automated cell countess (Invitrogen), by using Trypan Blue. To normalize the data, the counted DFATs number obtained by the uncoated surface was used as a control to compare the other condition's cell number.

2.2.7 Flowcytometry analysis of DFATs

To characterize the phenotype of DFATs, flow cytometry analysis was performed. Cells were detached with Trypsin/EDTA, then incubated on ice for 30 min in PBS with 10% FBS. Then, cells were centrifuged for 1 min at 3500 rpm. At least 2.5x10^5 cells per Eppendorf tube incubated with the APC-conjugated monoclonal antibodies against CD44, CD73, CD90 and CD105 or the respective isotype control (1/50, in 1% BSA in PBS) on ice for 45 min in the dark. After washing steps, the labeled cells were analyzed by BD FACSMelody™ flowcytometer and FlowJo software.

2.2.8 Polymer and protein coating on cell culture flasks

Collagen type I solution (AteloCell IPC50, the product concentration: 5 mg/mL) was diluted as 125 µg/mL with PBS (pH: 7.4). Collagen type IV and fibronectin solutions were prepared in PBS (pH: 7.4) at 125 µg/mL and 62.5 µg/mL. To ensure the solubility of collagen type IV, the stock solution was incubated at 4°C in a refrigerator until dissolving. The inner top surfaces of polystyrene (PS) cell culture flasks (surface area 12.5 cm^2) were then coated with 10 µg/cm^2, 10 µg/cm^2 and 5 µg/cm^2 of collagen type I, collagen type IV and fibronectin, respectively, for 1 h at room temperature, based on the recommended coating protocols of these proteins. A laminin solution was prepared in PBS (pH: 7.4) at 12.5 µg/ml on ice and PS flasks were coated at 1 µg/cm^2 at 4°C, overnight. For the coating of cationic (PLL, PDDA and PAH) and anionic (gelatin and gellan gum) polymers, PS flasks were coated with a sterile aqueous solution of PLL solution by following the provider's protocol, for 5 min at room temperature, with 8.33 µg/cm^2 polymer coated on the PS surface. PAH, PDDA, gelatin and gellan gum solutions were prepared in PBS (pH: 7.4) and PS flasks were coated by following the same concentrations as the PLL coating procedures, also for 5 min, at room temperature. After all the incubations, flasks were washed with PBS (pH: 7.4) three times. All coating procedures were performed inside a laminar flow hood to minimize contamination. A schematic representation of our study is shown in Fig. 1.

2.2.9 Water contact angle measurements

Contact angles of protein and polymer coated PS surfaces were measured by the sessile drop method (n=3). PS microscope slides (2.5×7.5 cm^2) were used as a substrate for the wettability measurements and were coated using the same conditions as for the PS cell culture flasks coating with each polymer and protein. Using a 19 G micro syringe, photographs were captured when the 5 µL Milli-Q water droplets met the surface. The images were then processed by FAMAS software with a Kyowa Contact Angle meter.

2.2.10 Zeta potential measurements of coating solutions

Zeta potential of proteins and polymer solutions were measured by a Malvern ZetaSizer. Disposable folded capillary cells were filled with coating solutions prepared in PBS (pH:7.4) as 800 µL and dynamic light scattering at 25°C (n=3).

2.2.11 Adsorbed protein assessment on uncoated and cationic polymer coated PS surfaces

To evaluate the amount of adsorbed serum protein on the uncoated PS plates, 25 µL of DMEM high glucose (20% FBS, 1% Penicillin-Streptomycin) were added onto 96-well plates. The plates were then incubated at 37°C for 16 h. The total amount of adsorbed protein on each well was evaluated by bicinchoninic acid (BCA) assay. After incubation, the medium was aspirated and 200 µL BCA working solution was inserted into each well, then incubated for 30 min at 37°C. The optical density was determined with a microplate reader at a wavelength of 562 nm and compared to a standard curve using BSA as a standard protein. To evaluate the amount of adsorbed serum protein on cationic polymer coated PS surfaces, 96-well plates were coated by PLL, PDDA and PAH polymers with 8.33 µg/cm^2 coating concentrations for 5 min at room temperature. 25 µL of DMEM high glucose (20% FBS, 1% Penicillin-Streptomycin) were added on each polymer coated well. The plates were then incubated at 37°C for 0.5, 1, 3 and 16 h. At the end of each time point the medium was aspirated and a BCA assay was applied in the same manner as explained above.

2.2.12 Fluorescence labeled polymer and protein coating on cell culture dishes.

To confirm the long-term stability of polymer or protein coatings, PS cell culture plastics (96 well plate) were coated with FITC conjugated collagen type I, FAM conjugated collagen type IV, rhodamine conjugated laminin, rhodamine conjugated fibronectin, and FITC conjugated PLL by following the same coating concentrations and conditions on PS cell culture flasks, at 10 µg/cm^2, 10 µg/cm^2, 1 µg/cm^2, 5 µg/cm^2, and 8.33 µg/cm^2, respectively. After surface coating, protein and polymer coated plates were incubated with DMEM 20% FBS, 1% Penicillin-Streptomycin medium for 1 week in 37°C, 5% CO_2 incubator. At the end of the 1 week of incubation, the medium was removed and the surface washed with PBS. Subsequently, fluorescent intensity of coated surfaces was imaged using a FV3000 Confocal Laser Scanning Microscope (Olympus, Tokyo, Japan). Change of fluorescent signal intensity was measured by Image J software (Fiji, version for Mac OS X) for each coated PS 96 well plate on day 0 and day 7 to confirm the remaining polymers on the surface after 1 week of incubation.

2.2.13 Statistical analysis

Two-tailed *t*-tests were performed to determine significant differences between pairs of data sets. Error bars represent standard deviation. *p* values < 0.05 were considered significantly different and are represented as: * $p < 0.05$, ** $p < 0.01$, *** $p < 0.001$, **** $p < 0.0001$, and *N.S.* is not significant.

3. Results and discussion

3.1. Validation of DFATs

The first step was to set up the control condition of our study by making mature adipocytes adhere to the top surface of a PS flask filled with culture medium. During the dedifferentiation process, adipocytes morphologically changed from a perfectly spherical shape to a spindle-like shape, already apparent from day 3 (Fig. 2A and B), as previously reported in the literature.[8,24] This process occurs by actin remodeling after mature adipocytes adhere to the surface, resulting in dynamic cellular deformation and secreting of the cell lipid droplet. Thereby, the lipid secreting cell acquires a fibroblastic appearance by morphological rearrangements. According to current studies to explain the underlying mechanism mentioned that YAP/TAZ[23], Hippo, Hedgehog signaling pathways[24] which are known to be involved in cytoskeletal remodeling, play a role in this process. It has also been shown on mesenchymal stem cells (MSCs) that as YAP expression increases, the cell geometry accordingly acquires a more elongated shape.[31] Regarding this, actin myofibrils of obtained DFATs were visualized by F-actin immunostaining (Fig. 2C, Fig. S1, and Fig. S2). On the other hand, while the mature adipocytes transform into DFAT cells, they express the stem cell markers Oct-4, Sox2, c-Myc and Nanog and obtained MSC-like properties.[32] Cytoplasmic Oct-4 expression of DFATs was thus shown to validating the DFATs stemness, additionally with stained actin myofibrils confirming typical of the cytoskeletal fibroblastic cell morphology in Fig. S1 with numerous stress fibers present in cells. Under the authority of International Federation of Adipose Therapeutics and International Society for Cellular Therapy, MSCs have to provide following surface antigen: CD44, CD73, CD90 and CD105[33]. According to flowcytometry analyzes performed with 3 parallels, obtained DFATs were positive for CD44, CD73, CD90 and CD105 (Fig. S3). This situation indicates that DFATs can reestablish multipotent characteristics and have MSC properties.[13] In light of this, the obtained cells in the present study with fibroblastic morphology, obtained by ceiling culture method for 1 week and counterstained with Hoechst, were confirmed to be DFATs with stem cell surface marker protein CD90 (pink color) and YAP (green color) located in the nuclei[31] (Fig. 2C). Since CD90 is one of the most analyzed surface markers for characterization of stem cells and DFATs[17,34,35], we checked it in our present report. To validate the multilineage differentiation capacity of DFATs, the cells were induced to differentiate into three distinct lineages: osteogenic, chondrogenic, and adipogenic. Following 21 days of osteogenic differentiation, we assessed the presence of calcium deposits in osteoblasts through Alizarin Red S staining. For chondrogenic differentiation, the production of proteoglycan compounds was detected using Alcian Blue staining on day 14. To confirm adipogenic differentiation, lipid droplets were visualized and stained with Oil Red O on day 14. (Fig. S4). Furthermore, as the regulation between the ECM and cell adhesion points and the actomyosin skeleton and shape is likely

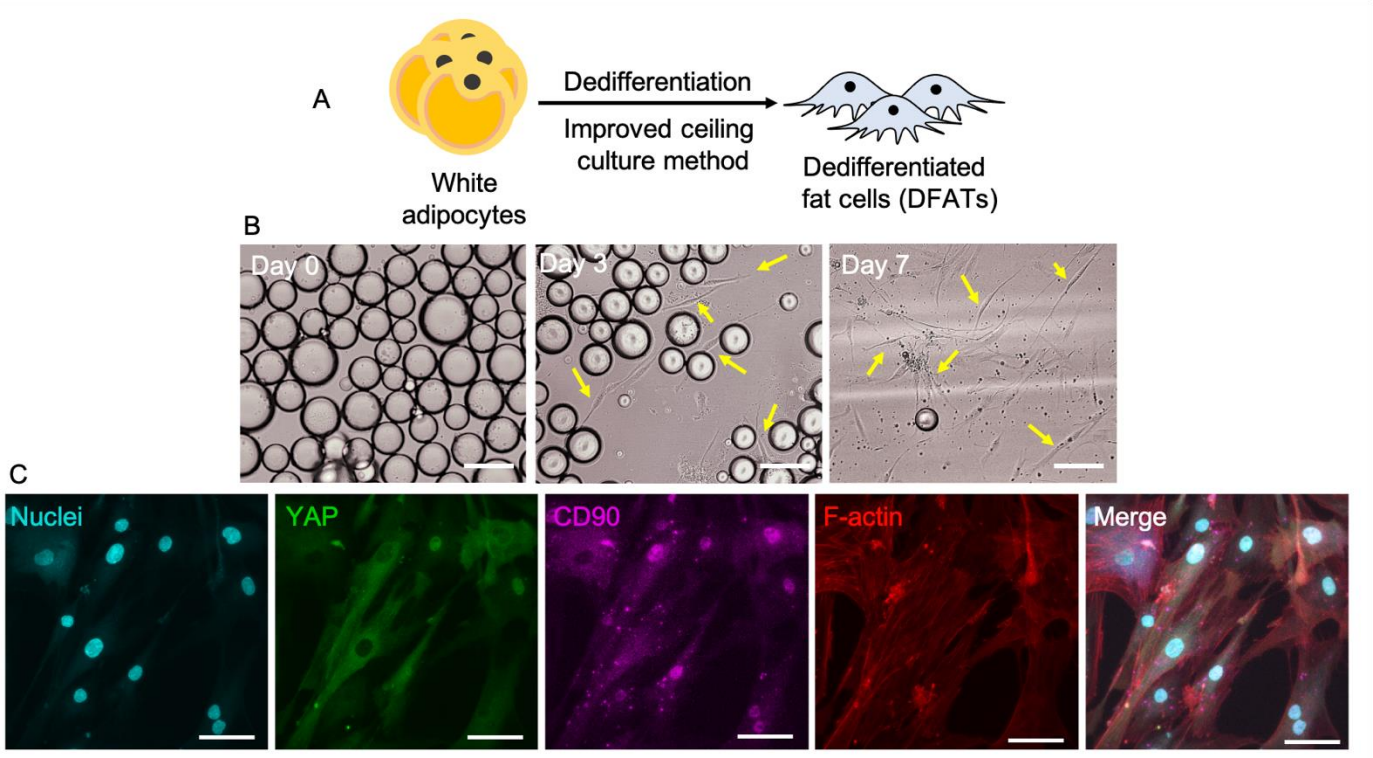

Fig. 2 A) Dedifferentiation of mature adipocytes. Differentiation process occurs after mature adipocyte attachment onto the surface and adipocytes lose their cytoplasmic fat content. As a result of the dedifferentiation, cells obtain fibroblastic cell morphology and stem cell properties with expressing CD90 surface marker and YAP. B) Upright microscope images of dedifferentiation process of mature adipocytes on day 0, 3 and 7. Yellow arrows represent the dedifferentiated fat cells on day 3rd and 7th. (Scale bar: 100 µm). C) Validation of DFATs. Immunofluorescence staining of CD90 (pink), YAP (green), actin myofibrils (red) of DFATs, and Hoechst counterstaining was used to visualize nuclei (blue) of DFATs on day 7. The colocalization of CD90, YAP, F-actin and nuclei of DFATs is shown in Merge image (Scale bar: 50 µm).

related to the previously mentioned Hippo, YAP and TAZ regulation and pathways [23,24,31], we can say that the confirmed expression of YAP in DFATs in our results (Fig. 2C) links the cell attachment and adhesion with the dedifferentiation process.

3.2. Optimization of ceiling culture medium

In our second step, we aimed to evaluate the effect of the serum concentration on the ceiling culture of mature adipocytes, comparing 0%, 10% and 20% (v/v) FBS in DMEM on obtaining DFAT cell ratio. FBS proteins are known to have the ability to be adsorbed on the surface, being potentially linked to the cell adhesion. The amount of adsorbed FBS proteins depending on the concentration was therefore monitored after 16 h of incubation on the uncoated PS surface, and was found to be 3.43 (± 2.68), 57.33 (± 1.67), 116.2 (±16.67) µg/mL of added culture medium respectively (Fig. 3A, gray bars). Moreover, DFAT cells obtained after 1 week of incubation in 0%, 10% or 20% were detached and the increased DFAT ratio was found with media containing 10% and 20% FBS (v/v) resulted in DFAT ratios of 1.45 (± 0.22) and 3.45 (± 0.25) (Fig. 3A, red bars). This result is consistent with the findings of Taniguchi et al., who reported that a significantly lower DFAT number was obtained with 10% FBS (v/v) when compared to ceiling cultures performed with 10% and 20% FBS (v/v).[36] Phase contrast images of DFAT cells in spindle shape geometry with increasing FBS concentration on the 7th day of culture are also seen in Fig. 3B. Furthermore, the viability of the cultured cells was evaluated by Live/Dead staining after 7 days of incubation. Hence, depending on the increased serum concentration, an increase was also observed in the number of viable cells (green color), while the number of dead cells (red color) was found to be lower (Fig. 3C). The obtained data indicate that FBS concentration is an important factor in obtaining DFAT as well as ensuring cell viability. Accordingly, 20% FBS was used in the subsequent experiments in this study.

While FBS, which is a supplement that promotes cell growth in basic cell culture studies, is generally added to the medium at a percentage of 2-10% (v/v), the use of culture media containing 10% (v/v) FBS[37], or 20% (v/v) FBS was used on DFAT ceiling cultures in the related reports.[6,14,38] Although the precise content of FBS is not known because it is an animal-derived product, Zheng et al. analyzed the protein concentration of three lots of FBS with proteomic techniques and reported that the protein amount was between 3.2 and 4.2 mg/mL.[39] On the other hand, Hong et al. found the protein concentration to be 4.1 mg/mL in DMEM high glucose medium containing 10% FBS by using the BCA method.[40] In this study, we measured the protein concentration of DMEM high glucose medium containing 0%, 10% and 20% (v/v) FBS with BCA assay as 1.09 (± 0.07), 3.66 (± 0.12), 4.65 (± 0.06) mg/mL, respectively (Fig. S5). The cell adhesion-enhancing effect of FBS (also called the "serum spreading factor") has been well defined, especially with the

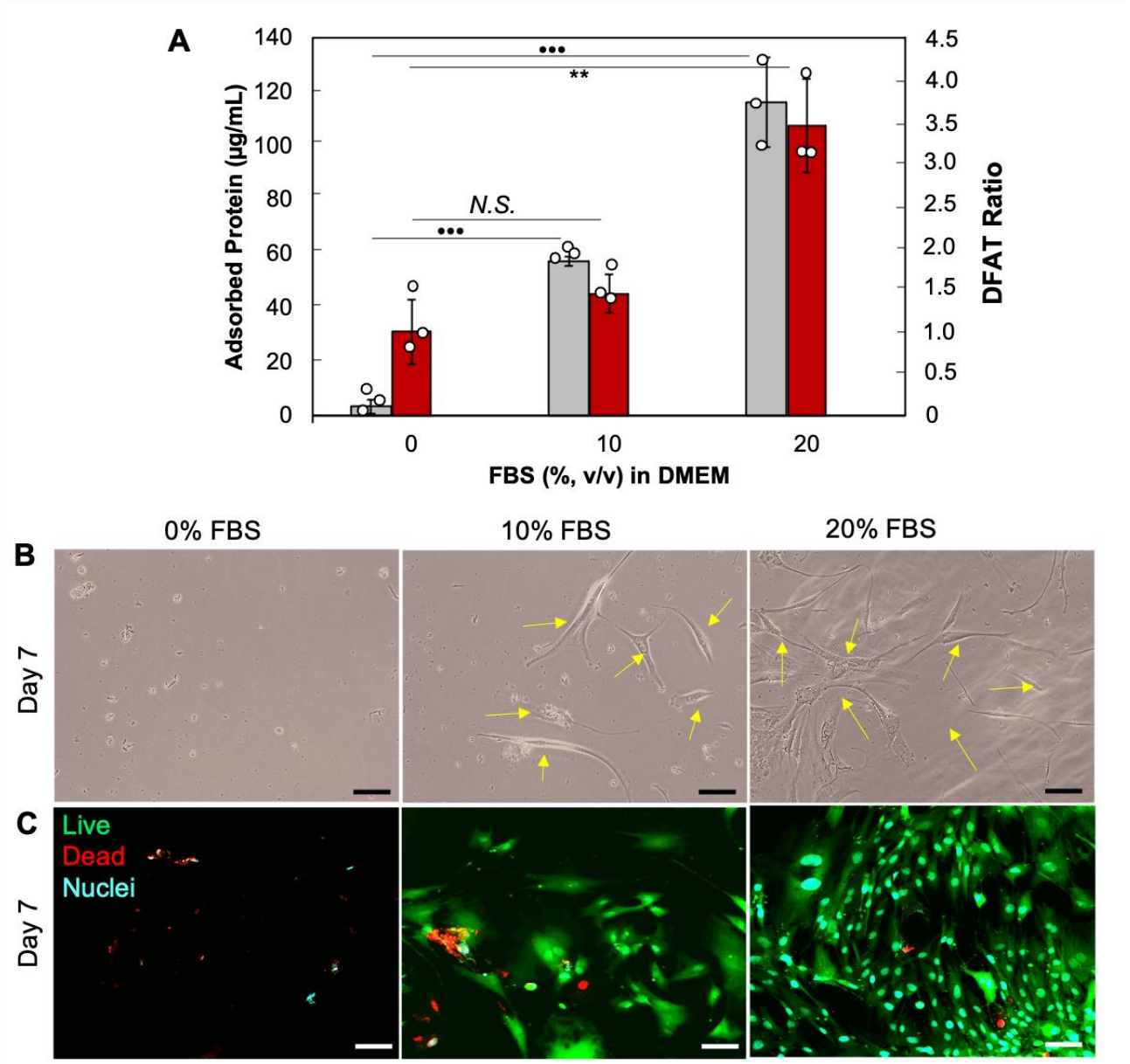

Fig. 3 Optimization of ceiling culture medium. A) Obtained DFAT rate (red bars) after 1 week of ceiling culture with 0%, 10% and 20% FBS (v/v) included DMEM high glucose medium. To normalize the data, obtained DFAT cell number by DMEM w/o FBS used as control to compare the other conditions' obtained DFAT cell number. The amount of absorbed protein (gray bars) on uncoated PS surfaces after 16 hours of incubation with 0%, 10% and 20% FBS (v/v) included DMEM high glucose. Statistically significant differences are stated by symbols: $^{**}p<0.001$ when the control group is DFAT ratio obtained by DMEM included 0% FBS (v/v) and $\bullet p<0.01$, $\bullet\bullet p<0.001$ when the control group is coating with DMEM included 0% FBS (v/v). *N.S.*: Not significant, n=3. B) Phase contrast images DFATs in ceiling culture with different FBS included medium on day 7. Yellow arrows indicate DFATs with their fibroblastic morphology (scale bar: 100 µm). C) Live&Dead images of DFATs on day 7 with 0%, 10% and 20% FBS (v/v) included DMEM high glucose medium, and Hoechst counterstaining was used to visualize nuclei (blue) of DFATs (scale bar: 100 µm).

fibronectin and the vitronectin proteins.[28,41] It is known that serum proteins in a cell culture medium can be adsorbed on the plastic cell culture dishes and cannot be completely removed by general washing steps.[40] FBS proteins are rapidly adsorbed on the substrate surface, and then cells adhere to this adsorbed protein layer so *in vitro* cell adhesion on any material is strongly due to these proteins.[42] Therefore, serum proteins may contribute to dedifferentiation by increasing cellular adhesion, which is a crucial step for the dedifferentiation process, due to the proteins it contains that increase cellular adhesion. Concerning the FBS attachment proteins as reported in related studies, fibronectin and vitronectin concentrations in FBS were reported to be 0.03 mg/mL and 0.21 mg/mL respectively[41], with an adhesive activity of vitronectin in fresh serum 8-16 times higher than that of fibronectin.[28] On the other hand, it was shown that the peripheral cytoplasm of cells can expand more widely in presence fibronectin than vitronectin for surface-dependent cells in a related study on BHK cells.[41] These data indicate the importance of both serum proteins for cytoskeletal organization. Finally, FBS is a rich mixture of nutrients, hormones, and growth factors (EGF, PDGF, IGF, insulin, etc.). Therefore, cell attachment factors are necessary, not only for the attachment of surface-dependent cells, but also cell viability, growth and proliferation.

3.3. Hydrophobicity effect assessment on DFAT ratio

In order to increase the adhesion of the mature adipocytes to the surface and thus their dedifferentiation, PS surfaces were then coated with ECM proteins fibronectin and collagen type I, as well as BM proteins (collagen type IV and laminin) and cationic (PLL, PDDA, PAH) and anionic polymers (gelatin and gellan gum). ECM and BM proteins provide a binding framework for the adhesion and growth of cells *in vitro*[43] and related studies have shown that substrate surfaces coated with ECM coating promotes cellular adhesion and proliferation of skin, liver and skeletal muscle cells.[44] In the current study, we evaluated the correlation of the physicochemical surface properties of the coated PS surfaces with the obtained DFAT ratio. First, hydrophobicity or water wettability feature was evaluated within the scope of the target, being one of the important surface characteristics that can affect cell adhesion, proliferation and interaction.[45] For this reason, after coating with proteins and polymers on PS surfaces, the obtained wettability was evaluated by water contact angle (C.A.) measurement. Images taken for water C.A. from protein, cationic and anionic polymer coated surfaces are shown in Fig. 4A, D and G, respectively, with obtained values (Fig. 4B, E and H) (gray bars). DFAT cells obtained from the coated surfaces after 1 week of culture were measured (Fig. 4B, E, H, red bars). Accordingly, the C.A. of the uncoated PS surface was measured as 82° (± 2.6). The C.A. values of the protein-coated PS surfaces were 73° (± 5.4), 54° (± 2.9), 39° (± 6.0) and 39° (± 3.6), for laminin, fibronectin, collagen type IV and type I respectively (Fig. 4A, B). DFAT ratios showed higher results for laminin and collagen type I coated surfaces, with 2.98 (± 0.92) and 2.89 (± 0.84), DFAT ratios, respectively, while fibronectin and collagen type IV coated surfaces were 1.84 (± 0.43) and 2.41 (± 0.83) (Fig. 4B, red bars). It is known that the surface is considered to be hydrophobic if the C.A. value is between 150° and 90°, super hydrophobic if it is greater than 150°, hydrophilic if it is between 90° and 10°, and super hydrophilic if it is less than 10°.[45] In terms of cell adhesion and spreading, it has been stated in various studies that moderate hydrophobicity is more favorable.[46,47] Tamada et al. (1986) reported that maximum cell adhesion could be achieved when the C.A. value was around 70°, and cell adhesion was significantly reduced when it was less than 40° with the HeLa S3 cell line.[48] Altankov et al. showed that for the attachment of dermal fibroblasts, a C.A. value of 65° yielded the best cell attachment, and the lowest when it was 85°.[47] As such, it is understood that the C.A. values of the ECM and BM protein-coated surfaces varying between 54° and 73° degrees in this study provide a suitable substrate for cell adhesion and therefore for dedifferentiation of mature adipocytes. On the other hand, C.A. values of PS surfaces coated with cationic polymers were measured as 79° (± 1.9), 80° (± 1.8) and 91° (± 2.1) for PAH, PLL and PDDA, respectively (Fig. 4D and 4E, grey bars). Even though the cationic polymer coating resulted in relatively higher C.A. values, PLL and PDDA yielded relatively higher DFAT ratios than PAH. Coating with PAH resulted in a DFAT ratio of 1.27 (± 0.95), while PLL and PDDA yielded a DFAT ratio of 2.19 (± 0.91) and 2.27 (± 2.8), respectively (Fig. 4E, red bars). This result interestingly shows that, independent of hydrophobic effects, a cationic polymer coating may have an effect on the DFAT ratio due to reasons such as electrostatic interactions because the high C.A. values cannot fully explain the increased DFAT ratio.

On the other hand, for the anionic polymer coating, the C.A. values of gelatin and gellan gum coated surfaces were measured as 65° (± 3.5) and 90° (± 3.2), respectively (Fig. 4G and 4H, grey bars). They seem to have the opposite effect in terms of DFAT ratio with lower values obtained from gelatin and gellan coated surfaces of 0.85 (± 0.14) and 0.32 (± 0.12), respectively (Fig. 4H, red bars). These results show the positive impact of proteins and cationic polymers for cell attachment, compared to anionic polymers, but strengthen the possibility that other mechanisms, independent of surface hydrophobicity, may be effective in increasing or decreasing the DFAT ratio of the coating with charged polymers.

3.4. Electrostatic effect assessment on DFAT ratio

It has long been known that mammalian cell membranes have a net negative surface charge at pH 7. For example, this value has been reported to be -19.4 (± 0.8) mV, -31.8 (± 1.1) mV for Hela cells and erythrocytes, respectively.[49] Therefore, electrostatic attraction occurs between cells and positively charged surfaces, while electrostatic repulsion occurs between cells and negatively charged surfaces.[45] When it comes to the effect of the cationic polymer coating on increasing the DFAT ratio, it is highly likely that the electrostatic interaction between the coated surface and the negatively charged cell membrane may have an increasing effect on the DFAT ratio by increasing cellular attachment and adhesion. To evaluate this, the zeta potential values of the protein and polymer solutions that we used for surface coating were measured at pH 7.4 (Fig. 4C, F, I). Accordingly, the zeta potential values of PBS and fibronectin, collagen type IV, collagen type I, and laminin solutions prepared by diluting in PBS at pH 7.4 were -0.38 (± 0.46), -5.75 (± 0.36), -0.76 (± 0.39), -1.09 (± 0.26) and -6.57 (± 0.18) mV (Fig. 4C). For the cationic polymer solutions, zeta potentials were 7.7 (± 1.4), 11.2 (± 4.0), 13.5 (± 0.3) mV for PDDA, PLL and PAH, respectively (Fig. 4F). For the anionic polymers, gelatin and gellan gum yielded zeta potential values of -6.67 (± 0.51) and -16.7 (± 0.45) mV, respectively (Fig. 4I). In this case, it can be concluded that, since ECM and BM proteins have negative zeta potential values, their effect of increasing the DFAT ratio is probably not due to electrostatic interactions between cell and coated surface, but through biological mechanisms such as integrin interaction which are involved in cellular adhesion, as well as the active reorganization of actin myofibrils.

Related to the zeta potential values of the cationic polymers, PLL, PDDA and PAH increased the DFAT ratio by 2.19 (± 0.91), 2.27 (± 0.8) and 1.27 (± 0.95) times, respectively (Fig. 4E, red bars). Interestingly, although PAH gave the highest zeta potential value, it did not increase the DFAT ratio as much as PLL and PDDA. One of the strong possibilities for this result is that various polycations demonstrate cytotoxic effects in cell culture.[50] Kadowaki et al. reported that 15 min incubation of PAH at 0.02 mg/mL concentration had a strong

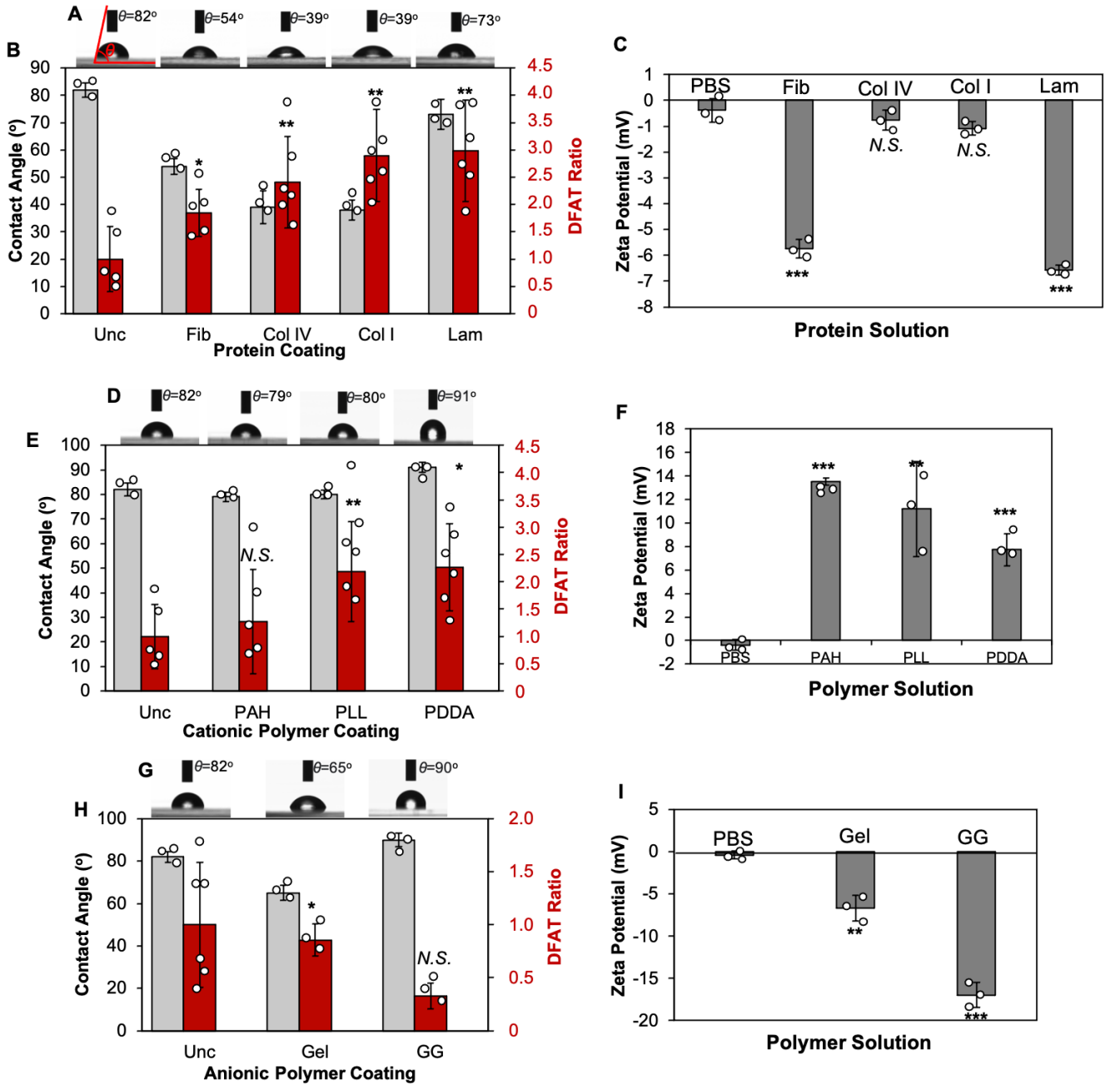

Fig. 4 Coating effect assessment of DFAT rate. Contact angle images of protein coated (A), cationic polymer coated (D) and anionic polymer coated (G) surfaces by sessile drop method performed on n=3. Contact angle values after coating (grey bars) and obtained DFAT cell numbers on protein coated (B), cationic polymer (E) and anionic polymer (H) coated surfaces (red bars). To normalize the data, obtained DFAT cell number by uncoated surface used as control to compare the other conditions' obtained DFAT cell number. Statistically significant differences are stated by symbols: *p<0.1, **p<0.01, and ***p<0.001 when the control group is DFAT ratio from uncoated PS surface. The graphs show results as means ± s.d. of experiments performed on n=6. Zeta potential measurements of protein (C), cationic polymer (F) and anionic polymer (I) solutions for coating. Statistically significant differences are stated by symbols: *p<0.01, **p<0.001 and, ***p<0.0001 when the control group is PBS (pH:7.4) (*N.S.*: Not significant). The graphs show results as means ± s.d. of experiments performed on n=3. (Unc: uncoated, Col I: Collagen I, Col IV: Collagen IV, Lam: Laminin, Fib: Fibronectin, PLL: Poly-L-lysine, PAH: Polyallylamine hydrochloride, PDDA: Polydiallyldimethylammonium chloride, Gel: Gelatin, GG: Gellan Gum).

cytotoxic effect on L929 fibroblasts.[51] Accordingly, the possible reason why we could not obtain a high DFAT ratio from PS surfaces coated with a PAH solution prepared as 0.1 mg/mL for 8.33 µg/cm^2 coating may be that PAH has a cytotoxic effect on mature adipocytes, similar to the one in the aforementioned report. To confirm this, Live/Dead assay was applied to DFATs seeded on PAH-coated PS surfaces on day 7 and cell viability was evaluated comparing with uncoated PS surfaces. Consequently, 50% significantly lower cell viability was observed on PAH-coated surfaces (Fig. S6) In fact, although the cytotoxic mechanisms of polycations are not fully elucidated, their conformational flexibility also plays a role in cell viability as well as their concentrations. Therefore, the stiffer structure of the ring system of a PDDA molecule prevents its attachment to the cell membrane[50,51], but is effective for the

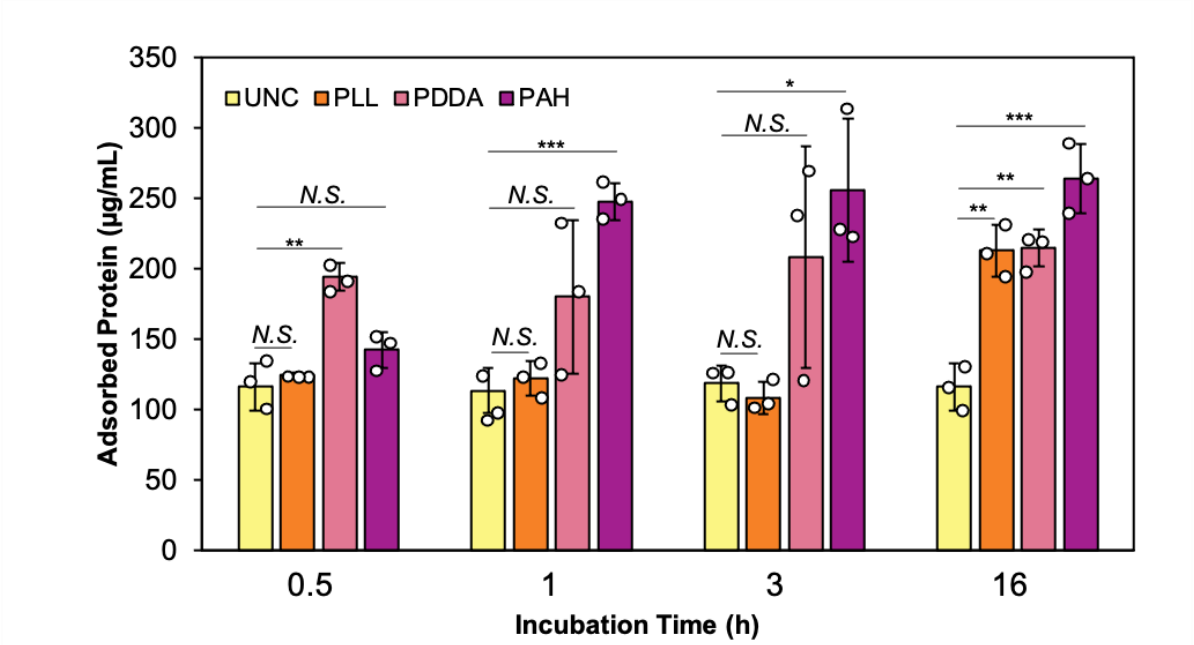

Fig. 5 Amount of adsorbed protein by DMEM (20% FBS) incubation on cationic polymer coated surfaces on different time points (n=3). Statistically significant differences are stated by symbols: *p<0.01, **p<0.001, *N.S.*: not significant. (UNC: Uncoated, PLL: Poly-L-lysine, PAH: Polyallylamine hydrochloride, PDDA: Polydiallyldimethylammonium chloride).

adsorption of serum proteins on the PS surfaces, thus making it less cytotoxic. Another reason for the increase of dedifferentiation on the cationic polymer coated surfaces is that coating with these polymers may have a promoting effect on the adsorption of serum proteins, which show a slightly negative zeta potential value, to the surface, while the situation is the opposite for anionic polymers, providing the necessary environment for cell attachment, spread and therefore dedifferentiation. To evaluate the adsorbing effect of serum proteins on the surfaces coated with cationic polymers, we incubated the polymer-coated surfaces with DMEM containing 20% FBS for 0.5, 1, 3, and 16 h, then a BCA assay was performed to measure the adsorbed proteins level (Fig. 5). The accumulated protein concentration on uncoated PS surfaces were found to be between 113.7 (± 16.2) and 118.7 (± 12.7) µg/mL, with no significant differences over the time (Fig. 5, yellow bars). This indicates that the maximum serum protein adsorption on uncoated PS surfaces occurs in less than half an hour. As a result of PLL coating, while the amount of adsorbed protein did not increase at other time intervals (values are not statistically significant), it reached a maximum at the end of 16 h of incubation and was found to be almost twice that of uncoated at 212.9 (± 18.8) µg/mL (Fig. 5, orange bars). The amount of adsorbed protein on PDDA-coated surfaces increased more than the other two groups at the mentioned time points and was found to be 194.3 (± 9.7), 180.3 (± 54.6), 208.4 (± 78.3), and 214.8 (± 13.0) µg/ml, respectively (Fig. 5, pink bars). On the surfaces covered with PAH, the amount of adsorbed protein after 0.5 h was slightly higher than in the uncoated and PLL-coated group, and was 142.6 (± 12.7) µg/mL, reaching the highest values for all time points among all other groups, measured as 247.4 (± 13.0), 255.9 (± 51.0) and 264.3 (± 24.6) µg/mL (Fig. 5, purple bars). These values are compatible with each other when the obtained zeta potential values of the cationic polymer solutions are considered (Fig. 4F). Indeed, the positively charged PDDA and PLL may have increased the cell adhesion by increasing serum protein adsorption on the surface and thus the cell interaction which should lead to an increased DFAT ratio. Accordingly, fibroblastic cell morphology was confirmed by F-Actin staining of DFATs cultured on PLL-coated surface (Fig. S1). However, although PAH has a higher effect of increasing serum protein adsorption, its cytotoxic effect may explain its limited increase found for the DFAT ratio, compared to PLL and PDDA. Based on these data, ceiling culture was also performed with PS surfaces coated with anionic polymers (gelatin, gellan gum) to confirm whether the electrostatic effect has an increasing or decreasing effect on mature adipocytes. The gelatin and gellan gum polymer solutions (Fig. 4I) had a zeta potential value of -6.67 (± 0.51) and -6.96 (± 1.45) mV, respectively. The number of DFAT cells associated was 0.86 (± 0.15) and 0.33 (± 0.12) for gelatin and gellan gum, respectively (Fig. 4H, red bars) and after 1 week of ceiling culture in gelatin and gellan gum coated PS flasks, mature adipocytes retained their smooth spherical shape (Fig. S3). It is highly probable that negatively charged surfaces reduced cell attachment and thus dedifferentiation by reducing the adsorption and adhesion of both positively charged serum proteins and cells to the surface. While the zeta potential of the gelatin-coated surface is slightly negative, it's not significantly lower than the other protein-coated PS surfaces. Therefore, it's less likely that electrostatic repulsion is the primary reason for the lower cell adhesion on the gelatin-coated surface. The conformation of adsorbed proteins is crucial. Even if two surfaces have similar zeta potentials, the arrangement of proteins and the exposure of binding sites can differ, affecting cell adhesion, as well as the uniformity or density of the protein coating. While surface charge can play a role in cell adhesion, it is unlikely to be the sole factor explaining the observed differences. Here it seems that DFAT can attach better on

proteins coatings through biological effect, using their integrins for instance, than thanks to surface charge.

morphology when subjected to ceiling culture for seven days on surfaces coated with gelatin and gellan gum (Fig S7). Huber et al.

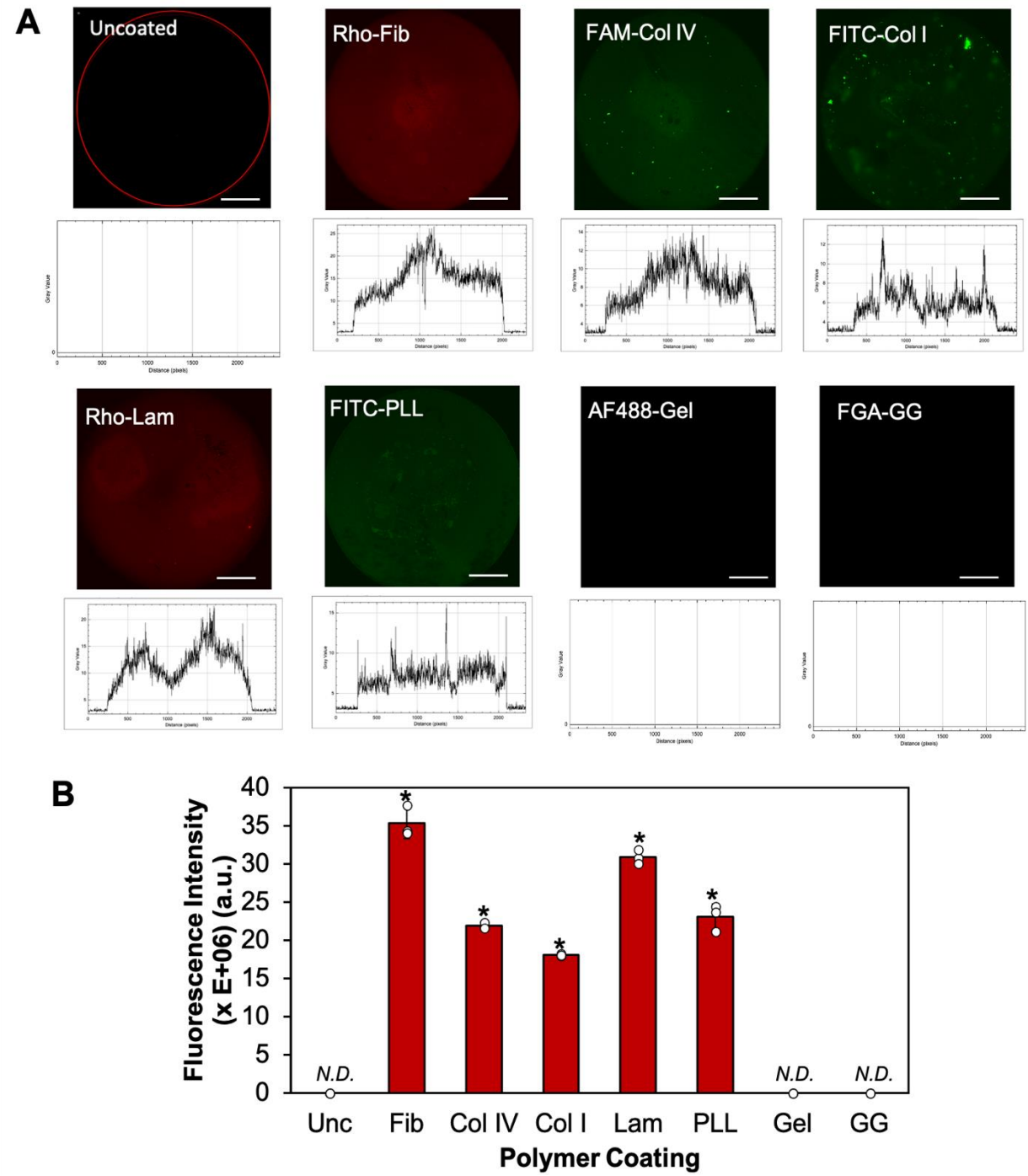

Fig. 6 Fluorescence labelled polymer coating on tissue culture polystyrene well plates. A) CLSM images, (Scale bar: 1mm), B) Fluorescence intensity values of fluorescence labelled polymer coated surfaces. When control group is fluorescence intensity of uncoated well plate surface, statistically significant differences are stated by symbols: *p<0.0001 (Unc: uncoated, Col I: Collagen I, Col IV: Collagen IV, Lam: Laminin, Fib: Fibronectin, PLL: Poly-L-lysine, Gel: Gelatin, GG: Gellan Gum, FGA: Fluoresceinyl glycine amide, FITC: Fluorescein isothiocyanate, FAM: 6-carboxyfluorescein, Rho: Rhodamine, AF488: Alexa Fluor 488, N.D. Non detected).

In fact, while both gelatin and gellan gum are biocompatible materials for *in vitro* cell cultures[52,53], it has been reported in various studies that they can actually be used for preserving mature adipocyte function instead or even for differentiating preadipocytes into adipocytes.[54,55] In relation to this matter, we noticed that fully developed fat cells predominantly retained their rounded

were then able to stably culture mature adipocytes encapsulated in methacrylated gelatin hydrogel for 2 weeks.[54] In other reports, human-derived stem cells encapsulated in gellan gum were also differentiated into mature adipocytes.[55,56] In other words, when these data and our findings are combined, it is concluded that these anionic polymers can be more favorable for the culture of mature

adipocytes without functional change or for adipocyte differentiation of precursor cells, rather than dedifferentiation.

3.5. Proteins and polymers amount effect assessment on DFAT ratio

Another possible explanation for the different effects of proteins and polymers on DFAT obtention could be found in the actual amount remaining on the surface after the coating. To visualize and evaluate this quantitatively, PS surfaces were coated with fluorescent labeled polymers and proteins (Fig. 6A). With the confocal microscope images obtained, the fluorescence intensity (F.I.) of the surfaces was quantified with Image J, confirming the coating of the surfaces with the relevant materials (Fig. 6B). As expected, no fluorescence could be obtained on uncoated surfaces. F.I. values obtained showed 35.4, 21.4, 18.1, 30.9, and 23.1 (xE+0.6) for fibronectin, collagen type IV, collagen type I, laminin and PLL, on day 7, respectively. Furthermore, to verify the enduring stability of the polymer coating over the one-week period of cell culture on the ceiling, we subjected PS surfaces treated with fluorescently labeled fibronectin, laminin, collagen I, collagen IV, and PLL to a 37°C incubation with DMEM containing 20% FBS for one week. Subsequently, after the one-week incubation, we removed the medium and washed the surfaces with PBS, followed by capturing fluorescence images (FI) using a confocal microscope. The comparison of FI values between day 0 and day 7 revealed that there are still remaining FI percentages of at least 70%. This finding confirms that the coated polymers remained stable on the surface, as shown in Figure S8. This stability is an important observation and suggests that the coatings effectively adhere to and maintain their integrity on the surface over the course of the experiment. However, F.I. could not be detected for anionic polymer coated PS surfaces, probably because the very thin coating was not observable even though it could still alter the FBS proteins adsorption and cell attachment. Although the F.I. method is not a highly sensitive technique, it can be said that these polymers are coated on the surface, albeit at the molecular level, since the anionic polymer coating has an effect on the DFAT ratio probably coming resulting from an inhibition of FBS proteins adsorption or directly limiting cell attachment. Although the fibronectin coating gave the highest F.I. value and therefore more adsorbed protein, it resulted in a DFAT ratio of 1.84 (± 0.43), lower than laminin and collagen type I coating with 2.98 (± 0.92) and 2.89 (± 0.84), respectively. The difference of adsorbed FBS proteins itself cannot therefore fully explain the difference of DFAT ratio observed which confirms that it may finally be linked to an aspect of cellular response, such as cell attachment specific integrins binding.

Conclusions

From this study, proper cell attachment appeared very important for dedifferentiation of mature adipocytes. According to our results, there are several possible reasons for the increase in the rate of cell attachment and obtaining DFATs. First of all, FBS containing vitronectin and fibronectin, also known as a serum spreading factor for cell adhesion, may have increased the DFAT ratio by increasing the adhesion of mature adipocytes on the cell culture dish (Fig. 7A). The attached cells reorganize the cytoskeleton via actin myofibrils, expels the lipid droplet out of the cell, and transforms into DFAT, which is characterized by a fibroblastic appearance. Secondly, coating with ECM and BM proteins may have increased dedifferentiation by increasing both the adsorption of mature adipocytes and the serum proteins on the surface (Fig. 7B). Especially laminin showing the highest effect with a DFAT ratio of 2.98, as well as PLL and PDDA, cationic polymers, which increased the DFAT rate by approximately 2.2 times. Additionally, the obtained DFAT share the same stemness markers expression CD44, CD73, CD90 and CD105, as confirmed by flow cytometry analyzes (Fig. S3). This situation indicates that these DFATs can reestablish multipotent characteristics and have MSC properties in the same way.[13] Therefore, cytoskeleton reorganization occurred and dedifferentiation could be achieved. On one hand, coating with cationic polymers may have increased the adsorption of serum proteins to the surface, thereby increasing the adhesion of mature adipocytes and thus the DFAT ratio (Fig. 7C). In this process, electrostatic interactions due to a negatively charged cell membrane and positively charged polymer coating, as well as integrin-mediated biological mechanisms, are strong possible causes. On the other hand, coating with anionic polymers might have reduced the DFAT ratio by reducing both the adhesion of the negatively charged cell membrane to the surface and the adsorption of serum proteins, with a similar electrostatic interaction logic (Fig. 7D). In attempt to summarize and conclude about both hydrophobic effect and electrostatic effects on cellular adhesion and dedifferentiation, while it can be thought that the dedifferentiation rate on protein-coated surfaces is related to a linear correlation with the surface hydrophobicity the relationship between hydrophobicity and electrostatic effect is not easy to assess. It seems that to maximize mature adipocytes adhesion and thus DFAT yield, it's more important to actually find the right balance. On one hand, extremely hydrophobic surfaces mean high protein adsorption which helps for cell attachment up to an excessive protein adsorption which will instead alter the cell adhesion. On the other hand, electrostatic effects, which can be controlled through surface charge modification, such as by altering the charge density or by specific functional groups that influence charge distribution, thus depending on how the proteins will be adsorb, may also finally affect their conformation positively or negatively. To optimize it, we need to find the right conditions for proteins to adsorb in a limited way that promotes their proper conformation and enhances cell adhesion. Then, cell adhesion, not only for DFATs but also for other anchorage-dependent cells such as mesenchymal, epithelial or endothelial cells, is vital and involves the following hierarchical steps. At the molecular level, integrin-mediated cell-ECM or cell-substrate adhesion are the main substrate of adhesion receptors, directly linking ECM or the surface to cytoskeletal adapters. Thus, the bundling of actin filaments is promoted by stretch-induced changes in actin filament conformation.[31] Therefore, ECM and BM proteins are often used to coat the surface or scaffold thanks to their effects on increasing cell

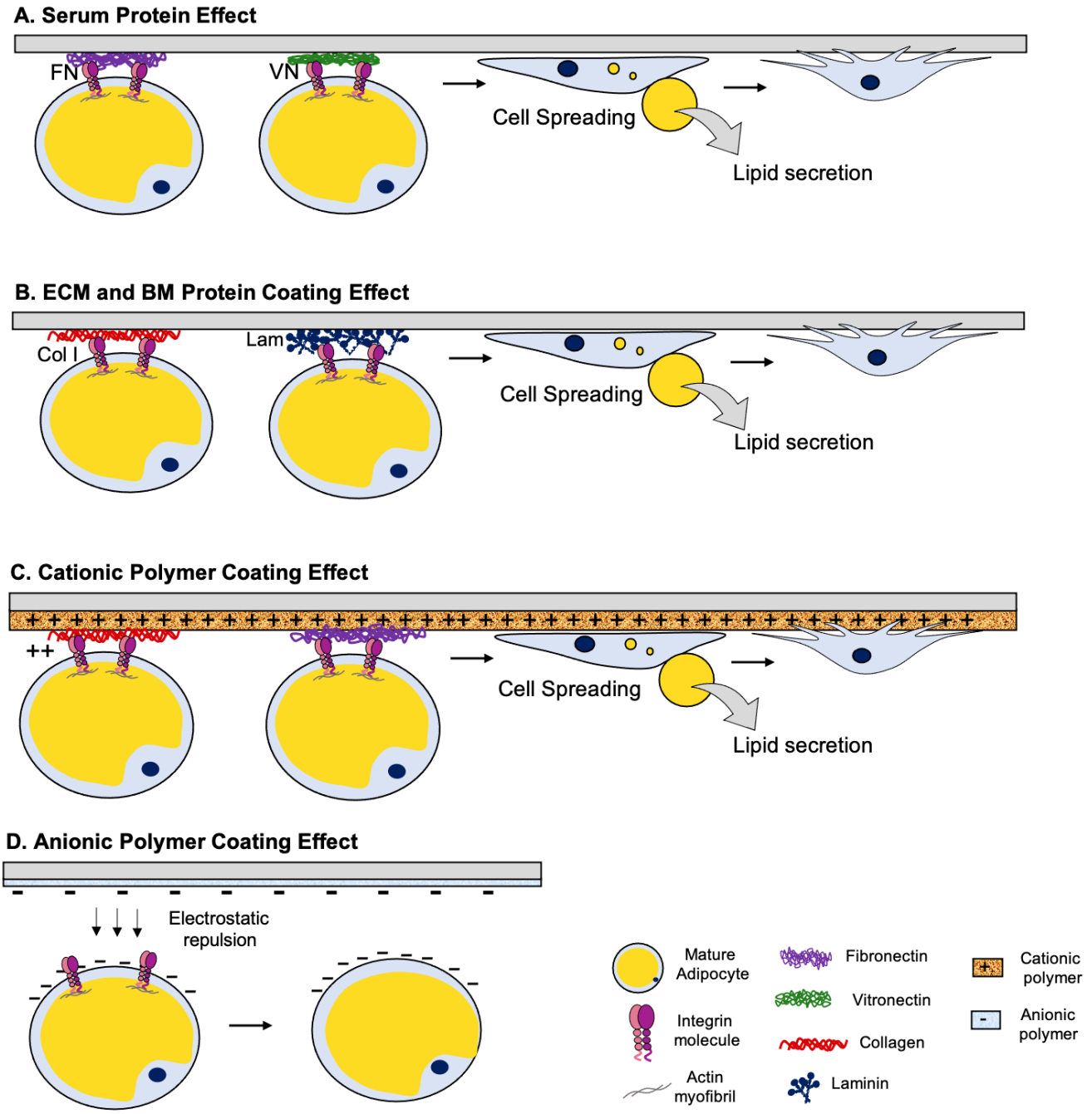

Figure 7. Expected biological mechanism of polymer coating effect on dedifferentiation of mature adipocytes. A) Adsorbed serum proteins might increase mature adipocyte attachment, thus increase DFAT ratio. B) Adsorbed ECM and BM proteins might increase mature adipocyte attachment, thus increase DFAT ratio. C) Electrostatic interaction between cell and coated surface might increase protein adhesion, thus cell attachment and DFAT ratio. E) Electrostatic repulsion between cell and surface might decrease the cell attachment and then dedifferentiation of mature adipocytes.

adhesion. Bellas et al. differentiated adipose derived MSCs into mature adipocytes with silk scaffolds by coating the scaffolds with laminin to increase the adhesion of cells to the scaffolds.[57] In addition, these proteins may also be effective for *in vitro* programming of adipocytes. Kamiya et al. indeed showed the inhibitory effect of mature adipocyte differentiation of preadipocytes cultured on fibronectin coated dishes[58], and the same was observed on collagen type I coated surfaces which upregulate of YAP expression.[59] These results raise the possibility that the proteins in question may be more suitable for dedifferentiation of mature adipocytes than the differentiation of progenitor cells into mature adipocytes or the maintenance of mature phenotypes in our case (Fig. 4F). For the adipocyte differentiation, dedifferentiation and cell fate, several integrins play a role during the processes. In a related study, it was reported that α5 expression is gradually diminished during adipogenesis, whereas α6 is increased in the differentiation

of 3T3-L1 preadipocyte into mature adipocytes.[60] In addition, another study reported a loss of β1-adrenergic receptors and an increase in β2- and β3-subtypes during terminal adipocyte differentiation.[61] It is known that αvβ3 integrin is involved in the interaction of vitronectin and fibronectin[62,63], as well as taking part in RGD-containing proteins (e.g. collagen type I, laminin).[62] It was also reported that αvβ3 maintains pluripotency by activating Wnt signaling in MSCs.[64] Thus, since activation of Wnt signaling leads to inhibition of PPARγ, which is involved in activating adipocyte differentiation, it can be hypothesized that αvβ3-mediated activation of Wnt signaling leads to subsequent adipocyte dedifferentiation.[65]

In conclusion, in this study, we aimed to control the adhesion and dedifferentiation of mature adipocytes to the surface by performing physicochemical surface modification using proteins and charged polymer coatings for adipocyte dedifferentiation. Our results revealed that the DFAT ratio can be increased on the surfaces coated with ECM and BM proteins and cationic polymers, while the anionic polymer coating may cause the opposite effect.

Author Contributions

A.S.K. carried out the experiments and wrote the manuscript. All authors edited the manuscript and contributed to design and implementation of the research with the analysis of results. All authors have given approval to the final version of the manuscript.

Conflicts of interest

There are no conflicts to declare.

Acknowledgements

This work was supported by a Grant-in-Aid for Scientific Research (A) (20H00665), Mirai-Program (18077228) from JST, a project (JPNP20004) subsidized by the New Energy and Industrial Technology Development Organization (NEDO), and collaborating research fund from Meiji Co., Ltd. and The Food Science Institute Foundation (J211061161). The author acknowledges financial support from the Japanese Government (Monbukagakusho: MEXT) Scholarship. The fee of English grammatical proof of this manuscript was paid by Meiji Co., Ltd. and The Food Science Institute Foundation (J211061161).

Notes and references

1 F. Louis and M. Matsusaki, Adipose tissue engineering, *Biomater. Organ Tissue Regener.,* 2020, 393-423, DOI: 10.1016/B978-0-08-102906-0.00008-8.

2 S. Niemala, S. Miettinen, J. R. Sarkanen and N. Ashammakhi, *Tissue Eng*., 2008, **4**, 1-26.

3 E. D. Rosen and O. A. MacDougald, *Nat. Rev. Mo.l Cell Bio.l*, 2006, **7**, 885–896. DOI: 10.1038/nrm2066.

4 B. D. Pope, C. R. Warren, K. K. Parker and C. A. Cowan, *Trends Cell Biol.*, 2016, **26**, 745–755. DOI: 10.1016/ j.tcb.2016.05.005.

5 A. Sakers, M. K. de Siqueira, P. Seale and C. J. Villanueva, *Cell*, 2022, **185**, 419-446. DOI: 10.1016/j.cell.2021.12.016.

6 T. Matsumoto, K. Kano, D. Kondo, N. Fukuda, Y. Iribe, N. Tanaka, Y. Matsubara, T. Sakuma, A. Satomi, M. Otaki, J. Ryu and H. Mugishima, *J. Cell. Physiol.*, 2008, **215**, 210–222. DOI: 10.1002/jcp.21304.

7 M. Jumabay, K. I. Boström, *World J. Stem Cells*, 2015, **26**, 1202-1214. DOI:10.4252/wjsc.v7.i10.1202.

8 X. Peng, T. Song, X. Hu, Y. Zhou, H. Wei, J. Peng and S. Jiang, *Biomed. Res. Int*, 2015, **2015**. DOI:10.1155/2015/673651.

9 M. F. Pittenger, A. M. Mackay, S. C. Beck, R. K. Jaiswal, R. Douglas, J. D. Mosca, M. A. Moorman, D. W. Simonetti, S. Craig and D. R. Marshak, *Science,* 1999, **284**, 143-147. DOI: 10.1126/science.284.5411.143.

10 L. Prantl, A. Eigenberger, E. Brix, S. Kempa, M. Baringer and O. Felthaus, *Cells*, 2021, **10**, 1113. DOI:10.3390/cells10051113.

11 H. Fujimaki, H. Matsumine, H. Osaki, Y. Ueta, W. Kamei, M. Shimizu, K. Hashimoto, K. Fujii, T. Kazama, T. Matsumoto, Y. Niimi, M. Miyata and H. Sakurai, *Regen. Ther.*, 2019, **11**, 240–248. DOI: 10.1016/j.reth.2019.08.004.

12. Z. Liang, Y. He, H. Tang, J. L;l, J. Cai, Y. Liao, *Stem Cell Res. Ther.* 2023, **14**, 207. DOI:10.1186/s13287-023-03399-0.

13. E. Watson, N. A. Patel, G. Carter, A. Moor, R. Patel, T. Ghansah, A. Mathur, M. M. Murr, P. Bickford, L. J. Gould and D. R. Cooper, *Adv. Wound Care,* 2014, **3**, 219–228. DOI: 10.1089/wound.2013.0452.

14 H. Fujimaki, H. Matsumine, H. Osaki, Y. Ueta, W. Kamei, M. Shimizu, K. Hashimoto, K. Fujii, T. Kazama, T. Matsumoto, Y. Niimi, M. Miyata and H. Sakurai, *Regen Ther.*, 2019, **11**, 240–248. DOI: 10.1016/j.reth.2019.08.004

15 T. Kazama, M. Fujie, T. Endo and K. Kano, *Biochem. Biophys. Res. Commun*, 2008, **377**, 180-185. DOI:10.1016/j.bbrc.2008.10.046.

16 M. Shimizu, T. Matsumoto, S. Kikuta, M. Ohtaki, K. Kano, H. Taniguchi, S. Saito, M. Nagaoka and Y. Tokuhashi, *J. Orthop Sci.*, 2018, **23**, 688-696. DOI:10.1016/j.jos.2018.03.001.

17 T. Yanagi, H. Kajiya, S. Fujisaki, M. Maeshiba, A. Yanagi-S, N. Yamamoto-M, K. Kakura, H. Kido and J. Ohno, *Regen. Ther.*, 2021, **18**, 472-479. DOI:10.1016/j.reth.2021.10.004.

18 X. Hu, P. Luo, X. Peng, T. Song, Y. Zhou, H. Wei, J. Peng and S. Jiang, *Gen. Comp. Endocrinol.*, 2015, **214**, 77-86. DOI:10.1016/j.ygcen.2015.01.016.

19 H. Sugihara, N. Yonemitsu, S. Miyabara and K. Yun, *Differentiation*, 1986, **31**, 42-49. DOI:10.1111/j.1432-0436.1986.tb00381.x.

20 J. A. Côté, J. Lessard, M. Pelletier, S. Marceau, O. Lescelleur, J. Fradette and A. Tchernof, *FEBS Open Bio.*, 2017, **7**, 1092-1101. DOI:10.1002/2211-5463.12250.

21 M. J. Harms, Q. Li, S. Lee, C. Zhang, B. Kull, S. Hallen, A. Thorell, I. Alexandersson, C. E. Hagberg, X. R. Peng, A. Mardinoglu, K. L. Spalding and J. Boucher, *Cell Rep.*, 2019, **27**, 213-225.e5. DOI: 10.1016/j.celrep.2019.03.026.

22 J. Lessard, J. A. Côté, M. Lapointe, M. Pelletier, M. Nadeau, S. Marceau, L. Biertho and A. Tchernof, *J. Vis. Exp.*, 2015, **7**, 52485. DOI:10.3791/52485.

23 L. Liu, X. Liu, M. Liu, Y. Jihu, D. Xie and H. Yan, *Exp Cell Res*, 2022, **415**, 113109. DOI: 10.1016/j.yexcr.2022.113109.

24 J.Kim,K.Y.Park,S.Choi,U.H.Ko,D.S.Lim,J.M.Suhand J. H. Shin, *Lab Chip*, 2022, **22**, 3920–3932. DOI:10.1039/d2lc00428c.

25 F. Wang, V. Zachar, C. P. Pennisi, T. Fink, Y. Maeda and J. Emmersen, *Int. J. Mol. Sci*, 2018, **19**, 517. DOI:10.3390/ijms19020517.

26 L. Liu, M. Liu, D. Xie, X. Liu and H. Yan, *Differentiation*, 2021, **122**, 1-6. DOI: 10.1016/j.diff.2021.11.001.

27 J. Ma, J. Xia, J. Gao, F. Lu and Y. Liao, *Plast. Reconstr. Surg.*, 2019, **144**, 1323-1333. DOI:10.1097/PRS.0000000000006272.

28 E. G. Hayman, M. D. Pierschbacher, S. Suzuki and E. Ruoslahti, *Exp Cell Res*, 1985, **160**, 245-258. DOI:10.1016/0014-4827(85)90173-9.

29 J. G. Steele, C. L. McFarland, B. Ann Dalton, G. Johnson, M. D. M. Evans, C. Rolfe Howlett and P. Anne Underwood, *J. Biomater. Sci. Polym. Ed*, 1993, **5**, 245-257. DOI:10.1163/156856293X00339.

31. J. emy Dufau, J. X. Shen, M. Couchet, T. de Castro Barbosa, N. Mejhert, L. Massier, E. Griseti, E. Mouisel, E. Z. Amri, V. M. Lauschke, M. Ryden and D. Langin, *Am. J. Physiol. Cell Physiol.*, 2021, **320**, C822-C841. DOI:10.1152/ajpcell.00519.2020.

31 G. Halder, S. Dupont and S. Piccolo, *Nat. Rev. Mol. Cell Biol.*, 2012, **13**, 591-600. DOI: 10.1038/nrm3416.

32 W. Gao, X. Qiao, S. Ma and L. Cui, *J. Cell Mol. Med.*, 2011, **15**, 2575–2585. DOI: 10.1111/j.1582-4934.2011.01313.x.

33 P. Bourin, B. A. Bunnell, L. Casteilla, M. Dominici, A. J. Katz, K. L. March, H. Redl, J. P. Rubin, K. Yoshimura and J. M. Gimble, *Cytotherapy*, 2013, **15**, 641-648. DOI:10.1016/j.jcyt.2013.02.006.

34 T. Kakudo, N. Kishimoto, T. Matsuyama, Y. Momota, *Cytotechnology*, 2018, **70**, 949-959. DOI:10.1007/s10616-018-0193-9.

35 S. Kono, T. Kazama, K. Kano, K. Harada, M. Uechi and T. Matsumoto, *Vet. J.*, 2014, **199**, 88–96. DOI: 10.1016/j.tvjl.2013.10.033.

36 H. Taniguchi, T. Kazama, K. Hagikura, C. Yamamoto, M. Kazama, Y. Nagaoka and T. Matsumoto, *J Vis Exp.*, 2016, **113**. DOI:10.3791/54177.

37 Y. Ohta, M. Takenaga, Y. Tokura, A. Hamaguchi, T. Matsumoto, K. Kano, H. Mugishima, H. Okano and R. Igarashi, *Cell Transplant*, 2008, **17**, 877–886. DOI: 54 10.3727/096368908786576516

38 M. Jumabay, T. Matsumoto, S. ichiro Yokoyama, K. Kano, Y. Kusumi, T. Masuko, M. Mitsumata, S. Saito, A. Hirayama, H. Mugishima and N. Fukuda, *J. Mol. Cell Cardiol.*, 2009, **47**, 565–575. DOI: 10.1016/j.yjmcc.2009.08.004.

39 X. Zheng, H. Baker, W. S. Hancock, F. Fawaz, M. McCaman and E. Pungor, *Biotechnol. Prog.*, 2006, **22**, 1294-1300. DOI:10.1021/bp060121o

40 X. Hong, Y. Meng and S. N. Kalkanis, *J Biol Methods*, 2016, **3**, e51. DOI: 10.14440/jbm.2016.129.

41 Y. Miyamoto, M. Izumi, S. Ishizaka and M. Hayashi, *Cell Struct. Funct.*, 1989, **14**, 151-162. DOI: 10.1247/csf.14.151.

42 M. Verdanova, P. Sauerova, U. Hempel and M. H. Kalbacova, *Histochem. Cell Biol.*, 2017, **148**, 273–288. DOI:10.1007/s00418-017-1571-7.

43 E. M. Harnett, J. Alderman and T. Wood, *Colloids Surf. B Biointerfaces*, 2007, **55**, 90–97. DOI:10.1016/j.colsurfb.2006.11.021.

44 Y. Zhang, Y. He, S. Bharadwaj, N. Hammam, K. Carnagey, R. Myers, A. Atala and M. van Dyke, *Biomaterials*, 2009, **30**, 4021–4028. DOI:10.1016/j.biomaterials.2009.04.005.

45 M. Ferrari, F. Cirisano and M. Carmen Morán, *Colloids Interfaces*, 2019, **3**, 48. DOI:10.3390/colloids3020048

46 E. M. Harnett, J. Alderman and T. Wood, *Colloids Surf. B Biointerfaces*, 2007, **55**, 90–97. DOI:10.1016/j.colsurfb.2006.11.021.

47 G. Altankov, K. Richau and T. Groth, *Materialwiss Werkstofftech*, 2003, **34**, 1120–1128. DOI: 10.1002/mawe.200300699

48 Tamada, Y.; Ikada, Y., *Polymers in Medicine II*, 1986, 101- 115.

49 O. v. Bondar, D. v. Saifullina, I. I. Shakhmaeva, I. I. Mavlyutova and T. I. Abdullin, *Acta Naturae*, 2012, **4**, 78-81. DOI:10.32607/20758251-2012-4-1-78-81.

50 D. Fischer, Y. Li, B. Ahlemeyer, J. Krieglstein and T. Kissel, *Biomaterials*, 2003, **24**, 1121-1131. DOI:10.1016/S0142- 9612(02)00445-3.

51 K. Kadowaki, M. Matsusaki and M. Akashi, *Langmuir.*, 2010, **26**, 5670-5678. DOI:10.1021/la903738n.

52 S. Ullm, A. Krüger, C. Tondera, T. P. Gebauer, A. T. Neffe, A. Lendlein, F. Jung and J. Pietzsch, *Biomaterials*, 2014, **35**, 9755-9766. DOI:10.1016/j.biomaterials.2014.08.023.

53 J. Silva-Correia, B. Zavan, V. Vindigni, T. H. Silva, J. M. Oliveira, G. Abatangelo and R. L. Reis, *Adv. Healthc. Mater.*, 2013, **2**, 568-575. DOI:10.1002/adhm.201200256.

54 B. Huber, K. Borchers, G. E. M. Tovar and P. J. Kluger, *J. Biomater. Appl.*, 2016, **30**, 699–710. DOI: 10.1177/0885328215587450.

55 F. B. Albrecht, F. F. Schmidt, A. C. Volz and P. J. Kluger, *Gels*, 2022, **8**, 611. DOI:10.3390/gels8100611.

56 M. E. L. Lago, L. P. da Silva, C. Henriques, A. F. Carvalho, R. L. Reis and A. P. Marques, *Bioengineering*, 2018, **5**, 52. DOI:10.3390/bioengineering5030052.

57 E. Bellas, K. G. Marra and D. L. Kaplan, *Tissue Eng. Part C Methods*, 2013, **19**, 745–754. DOI: 10.1089/ten.TEC.2012.0620.

58 S. Kamiya, R. Kato, M. Wakabayashi, T. Tohyama, I. Enami, M. Ueki, H. Yajima, T. Ishii, H. Nakamura, T. Katayama, J. Takagi and F. Fukai, *Biochemistry*, 2002, **41**, 3270-3277. DOI:10.1021/bi015660a.

59 X. Liu, X. Long, Y. Gao, W. Liu, T. Hayashi, K. Mizuno, S. Hattori, H. Fujisaki, T. Ogura, S. Onodera, D. O. Wang and T. Ikejima, *J. Cel.l Physiol.*, 2020, **235**, 1821-1837. DOI:10.1002/jcp.29100.

60 J. Liu, S. M. DeYoung, M. Zhang, M. Zhang, A. Cheng and A. R. Saltiel, *Cell Metab.*, 2005, **2**, 165-177. DOI:10.1016/j.cmet.2005.08.006.

61 F. M. Gregoire, C. M. Smas and S. Sul, *Physiol. Rev.*, 1998, **78**, 783-780. DOI: 10.1152/physrev.1998.78.3.783.

62 M. A. Horton, *Int, J. Biochem, Cell Biol.*, 1997, **29**, 721-725. DOI:10.1016/S1357-2725(96)00155-0.

63 L. Wang, D. Pan, Q. Yan and Y. Song, *Protein Sci.*, 2017, **26**, 1124-1137. DOI:10.1002/pro.3163.

64 D. Liu, X. Kou, C. Chen, S. Liu, Y. Liu, W. Yu, T. Yu, R. Yang, R. Wang, Y. Zhou and S. Shi, *Cell Res.*, 2018, **28**, 918-933. DOI:10.1038/s41422-018-0070-2.

65 M. Nohawica, A. Errachid and M. Wyganowska-Swiatkowska, *Biomed. Rep.*, 2021, **15**, 70. DOI: 10.3892/br.2021.1446